Ultrafast X-Ray Science at the Advanced Light Source

R.W. Schoenlein[1], A.H. Chin[2†], H.H.W. Chong[3], R.W. Falcone[2], T.E. Glover[4], P.A. Heimann[4], S.L. Johnson[2], A.M. Lindenberg[2], C.V. Shank[1], A.A. Zholents[5], M.S. Zolotorev[5]

[1]Materials Sciences Division, Lawrence Berkeley National Laboratory, Berkeley, CA 94720 USA

[2]Department of Physics, University of California, Berkeley, CA 94720 USA

[3]Applied Science and Technology Graduate Group, University of California, Berkeley, CA 94720 USA

[4]Advanced Light Source, Lawrence Berkeley National Laboratory, Berkeley, CA 94720 USA

[5]Accelerator and Fusion Research Division, Lawrence Berkeley National Laboratory, Berkeley, CA 94720 USA

[†]Presently at Lawrence Livermore National Laboratory

Our scientific understanding of the static or time-averaged structure of condensed matter on the atomic scale has been dramatically advanced by direct structural measurements using x-ray techniques and modern synchrotron sources. Of course the structure of condensed matter is not static, and to understanding the behavior of condensed matter at the most fundamental level requires structural measurements on the time scale on which atoms move. The evolution of condensed-matter structure, via the making and breaking of chemical bonds and the rearrangement of atoms, occurs on the fundamental time scale of a vibrational period, ~100 fs. Atomic motion and structural dynamics on this time scale ultimately determine the course of phase transitions in solids, the kinetic pathways of chemical reactions, and even the efficiency and function of biological processes. The integration of x-ray measurement techniques, a high-brightness femtosecond x-ray source, femtosecond lasers, and stroboscopic pump-probe techniques will provide the unique capability to address fundamental scientific questions in solid-state physics, chemistry, AMO physics, and biology involving structural dynamics. In this paper, we review recent work in ultrafast x-ray science at the ALS including time-resolved diffraction measurements and efforts to develop dedicated beamlines for femtosecond x-ray experiments.

Time-Resolved Bragg Diffraction of Order–Disorder Transitions

Initial time-resolved x-ray experiments at the ALS have focus on order–disorder transitions in crystalline solids. The dynamics of such phase transformations are of fundamental scientific interest since they determine the genesis and evolution of new structural phases. The conventional description of simple first-order solid/liquid phase transitions in crystals is based on a thermal model, which assumes local thermal equilibrium among the vibrational modes and between the electronic and vibrational energy reservoirs. In such a model, the phase transition proceeds via energy transfer to the lattice in the form of heat. The thermal model then predicts that following optical excitation, a phase transition will evolve on the time scale determined by electron-phonon energy exchange, typically several picoseconds. Implicit in such a description is the assumption that excitation or energy deposition to the solid is slow compared to a vibrational period or to electron-phonon scattering times. However, ultrafast optical pulses can deposit energy on time scales that are short compared to electron-phonon interaction times; thereby creating electron temperatures well in excess of the underlying lattice temperature. Energy can even be deposited on time scales shorter than electron-electron scattering times (<100 fs), creating non-equilibrium (non-Fermi) electron distributions. Under such conditions, the thermal melting model breaks down, and new physical effects emerge.

Ultrafast energy deposition raises fundamental scientific questions about how phase transitions occur under nonequilibrium conditions, and specifically whether "melting" of a solid can occur on the time scale of a phonon period (i.e., before the vibrational modes reach thermal equilibrium above the melting temperature). Such a "plasma-annealing" model was originally proposed more than 20 years ago, in an attempt to explain pulsed-laser annealing of Si [1]. Since then, theoretical models have predicted that in covalent crystals, the promotion of a large fraction of electrons from bonding to anti-bonding states will sharply reduce the restoring forces between atoms, rendering the crystal structure unstable on the time scale of ~200 fs [2]. Under such conditions, disordering may proceed in a manner analogous to photodissociation in molecules. Recent *ab-initio* molecular-dynamics calculations for Si [3] predict that unique metastable

structural phases, with coordination that is substantially different from either the solid or equilibrium liquid phase, can result from such non-equilibrium conditions.

To date, ultrafast non-equilibrium phase transitions in crystals with diamond and zinc-blende lattice structure (Si, GaAs, and InSb) have been studied using a variety of indirect optical techniques. Recent optical experiments provide some evidence of laser-induced disordering in crystalline silicon on a time scale comparable to the phonon period (~70 fs) [4-6]. Nevertheless, because optical measurements do not provide direct information about the atomic positions and coordination, they are unable to address the fundamental scientific questions related to structural dynamics in this regime.

Femtosecond x-ray diffraction provides direct information about long-range atomic order in crystalline systems, and a number of research groups are beginning to apply time-resolved x-ray diffraction to investigate ultrafast phase transitions using a variety of short-pulse x-ray sources [7,8]. Early experiments in InSb made use of 300 fs x-ray pulses (at 30 keV) generated via Thomson scattering between a terawatt laser pulse and 50 MeV electrons from the ALS linac injector [9]. Time-resolved diffraction measurements made with this relatively low-flux source, shown in Figure 1, clearly elucidate the energy transfer dynamics to the lattice from the initial electron-hole plasma created by the optical pulse. The process of electron-phonon energy relaxation and the development of acoustic phonons from anharmonic optical phonons are manifest in the diffraction data as a distinct delay (~10 ps) in the onset of lattice expansion following laser excitation [10]. The resulting strain (lattice expansion: $\Delta d \sim 4$ mÅ) and strain propagation into the sample at the sound speed can be directly measured.

Investigation of non-thermal melting requires greater surface sensitivity, since the highest electron-hole densities (which are thought to drive this process) are occur in a thin surface layer. Time-resolved diffraction measurements in InSb using 7.5 keV x-rays (Figure 2) shows the first hint of non-thermal ultrafast disordering. A slight drop in the diffraction efficiency is observed within 1 ps of excitation, indicative of the formation of a disordered surface layer ~30 Å thick [10]. Because of the differences in x-ray attenuation lengths,. spectral measurements of the

Bragg peak show a distinction between this loss in diffraction efficiency and the strain propagation observed with 30 keV photons (as shown in Figure 1)

These experiments, and more recent measurements using x-ray pulses generated from a laser produced plasma [8,10], have provided the strongest indication yet of non-thermal disordering driven directly by a high-density electron-hole plasma. They raise important scientific questions about the kinetics of disordering in this non-equilibrium regime. At the same time, these measurements illustrate the severely limited capabilities of existing short-pulse x-ray sources. The enhanced x-ray brightness and temporal resolution provided by a synchrotron-based femtosecond x-ray source will enable a quantitative interpretation of such time-resolved diffraction measurements and will further enable complementary EXAFS measurements of short-range structural dynamics.

Recently, the Falcone group has developed a complementary approach for time-resolved diffraction measurements by applying an ultrafast x-ray streak camera detector [11] at an ALS bend-magnet beamline. The flux and energy resolution (narrow bandwidth) provided by a synchrotron beamline enable a direct observation of energy-coupling from an optically-created electron-hole plasma to coherent vibrational modes of the lattice in InSb [12]. Figure 3 (left) shows the strong sinusoidal modulation of the x-ray diffraction intensity due to a coherent acoustic phonon mode. These measurements indicate that below a given threshold laser fluence, the primary mechanism of energy transfer between hot carriers and the lattice is coherent acoustic phonon generation via deformation potential coupling and LO phonon decay.

The phonon dispersion relation (inset Figure 3) is measured by sampling acoustic phonons of different momentum by changing the angle of the crystal. Above threshold (Figure 3 right), it was found that the atoms no longer coherently oscillate around the equilibrium positions of the lattice. Instead they are driven into a disordered state where no atomic motion of long-range coherence (and thus no oscillation in the x-ray Bragg diffraction) can exist. This occurs on the time-scale of one-half of a phonon period, at which point the atomic displacement exceeds the Lindemann criterion of melting. The generation of large amplitude coherent phonons is

evidently an important step in non-thermal disordering of a crystalline lattice. However, present temporal resolution of x-ray streak cameras, and the limited capabilities of femtosecond x-ray sources prevent a more complete study. Important questions remain about the time scale and mechanism for the order/disorder transition, the local structure of the disordered state, and the dynamics of the re-crystallization.

Generation of Femtosecond X-rays from a Synchrotron

Time-resolved Bragg diffraction measurements are a first step in the developing field of ultrafast x-ray science. Time resolved EXAFS and XANES measurements on complex systems and molecules require substantially higher flux than is available from existing ultrafast x-ray sources. To that end, we have developed a novel technique for generating femtosecond x-rays from a synchrotron [13,14,15]. This technique is the basis for a femtosecond bend-magnet beamline that is presently being commissioned at the ALS, as well as a proposed femtosecond undulator beamline.

The time structure of synchrotron radiation is determined by the duration of the stored electron bunches (≈30 ps), and storage of ultrashort bunches is problematic due to instabilities arising from bunch-induced wakefields and coherent synchrotron radiation. However, femtosecond-duration electron bunches can exist in a storage ring for a limited time. Our approach is to create femtosecond time-structure on a long electron bunch by using a femtosecond laser pulse to modulate the energy of an ultrashort slice of the bunch.

Figure 4 illustrates the modulation and generation scheme. A femtosecond laser pulse co-propagates with the stored electron bunch through a wiggler (Figure 4A). The high electric field of the laser pulse (~10^9 V/m) modulates the energy of the underlying electrons as they traverse the wiggler (electrons are accelerated or decelerated depending on the optical phase, ϕ, seen by each electron at the entrance of the wiggler). The optimal interaction occurs when the central wavelength of the spontaneous emission from an electron passing through the wiggler, $\lambda_S=\lambda_W(1+K^2/2)/2\gamma^2$, satisfies the resonance condition $\lambda_S=\lambda_L$ where λ_L is the laser wavelength,

and λ_W is the wiggler period. In addition, the transverse mode of the laser beam must match the transverse mode of the spontaneous radiation from the electron passing through the wiggler, and the laser spectral bandwidth must match the spectrum of the fundamental wiggler radiation averaged over the transverse mode. Under these conditions, the electron energy modulation, ΔE, is given by [13,14,15]

$$\Delta E = 2\left(A_L A_W \frac{M_W}{\sqrt{2} M_L} \eta_{emit} \right)^{1/2} \cos\phi \qquad (1)$$

where A_L is the laser pulse energy, M_W is the number of wiggler periods, M_L is the laser pulse length in optical cycles (FWHM), $A_W \cong 4.1\alpha hc/\lambda_L K^2/(2+K^2)$ is the energy spontaneously radiated by a single electron passing through the wiggler, and $\eta_{emit} \approx 0.7$ accounts for the non-zero electron beam size. For example: a 25-fs laser pulse with a photon energy of 1.55 eV, and a pulse energy A_L=100 μJ will produce an energy modulation amplitude $\Delta E \approx 9$ MeV using a wiggler of 19 periods.

By creating an energy modulation that is significantly larger than the beam energy spread, the transverse dispersion of the storage ring will cause a spatial displacement of the modulated electrons from the rest of the electron bunch (Figure 4B). Finally, by imaging the synchrotron radiation from the displaced electrons to the experimental area, femtosecond x-rays can be separated from the long-pulse using an aperture (Figure 4C). The duration of the synchrotron radiation produced by the laser-modulated electrons will be approximately the same as the laser pulse duration. Furthermore, the extraction of an ultrashort slice of electrons leaves behind an ultrashort hole or "dark pulse" in the core of the electron bunch. This dark pulse will appear in the generated x-rays, and can also be used for time-resolved spectroscopy.

Proof-of-principle experiments have been conducted at the ALS storage ring operating at E=1.5 GeV (rms beam energy spread σ_E=1.2 MeV) using a wiggler with M_W=19 periods, λ_W=16 cm, with the gap adjusted for K≅13. Femtosecond pulses (τ_L=100 fs, A_L=400 μJ, λ_L=800 nm, f_L=1 kHz,) from a Ti:sapphire laser system are synchronized to the

storage-ring RF using phase-locking techniques and are directed into the main vacuum chamber where they co-propagate with the electron beam through the wiggler. Following the interaction region, a mirror directs the fundamental spontaneous wiggler emission and the laser beam out of the storage ring to enable direct measurements of the temporal and spectral overlap and of the spatial mode matching between the laser pulses and the wiggler radiation. The efficiency of the laser–electron interaction is monitored by measuring the gain in the laser pulse energy. This gain ($\sim 10^{-3}$) is equivalent to the single-pass gain of a free-electron laser, and is optimum under the same mode-matching conditions described above.

The time structure of the temporally incoherent synchrotron radiation is directly determined by the time structure of the electron bunch and is invariant over the entire spectrum of the synchrotron emission, from infrared to x-ray wavelengths. We directly measure the time-structure of the visible synchrotron pulses (at ~2 eV) via cross-correlation (in BBO) with a delayed 50-fs pulse from the laser system. An adjustable knife-edge located in the beamline at an intermediate image plane provides a means to select synchrotron radiation originating from different transverse regions of the electron beam.

Figure 5 shows two cross-correlation measurements made at various knife-edge positions, in units of the rms horizontal beam size, σ_x. Measurements of the central core of the synchrotron beam (Figure 5A) reveal the femtosecond hole or dark pulse that is created by the acceleration (and deceleration) of electrons by the laser pulse and their subsequent transverse spatial separation from the central core of the bunch. The bright pulse is measured with the knife-edge at the $3\sigma_x$ position (Figure 5B) such that the central core of the beam is blocked. The solid lines in Figure 5 are predicted pulse shapes based on a model calculation of the electron bunch distribution (using known parameters of the electron beam and the storage-ring lattice) [14,15].

The location of the bend-magnet beamline used in these demonstration experiments is less than optimum because of the distance from the wiggler (in which the laser–electron interaction occurs) to the radiating bend magnet. Stretching of the laser-modulated electron bunch along this storage-ring arc accounts for the observed ~300fs pulse duration. For a bend-

magnet located immediately following the wiggler, the stretching of the electron bunch will be reduced by a factor of three, resulting in an x-ray pulse duration of ~100 fs.

The average flux and brightness of the femtosecond x-rays is determined by the full flux and brightness from an ALS bend-magnet (or undulator) beamline scaled by three factors: $\eta_1=\tau_L/\tau_e$, $\eta_2=f_L/f_B$, and $\eta_3\approx0.2$ where τ_L and τ_e are the laser pulse and electron bunch durations, f_L and $/f_B$ are the laser and electron-bunch repetition rates, and η_3 accounts for the fraction of electrons that are in the proper phase of the laser pulse to get the maximum energy exchange suitable for creating the large transverse separation. Synchrotron radiation damping provides for recovery of the electron beam between interactions. With a typical fill pattern of ~300 bunches in the storage ring, femtosecond x-rays can be generated at repetition rates as high as 100 kHz without adversely affecting the other beamlines at the ALS.

Figure 6 shows the calculated flux and brightness from two different femtosecond x-ray beamlines assuming a beam energy of 1.9 GeV, (400 mA average current, 30-ps bunch duration, 500-MHz repetition rate), and rms source size of 200 μm (H) × 20 μm (V) in the straight sections, and 100 μm (H) × 9 μm (V) in the bend sections. The first beamline (presently being commissioned at the ALS) is based on a bend magnet with a field of 1.27 T and an x-ray optic collecting 3 mrad (H) × 0.3 mrad (V) of the broadband bend-magnet emission. The expected x-ray pulse duration from this beamline is 100 fs (FWHM). The second beamline (proposed for ALS straight sector 6) is based on a small-gap undulator with 50 2cm periods and a maximum deflection parameter K of 2.02 (~5 mm minimum gap). This beamline is expected to generate 200-fs x-ray pulses and will form the basis of an Ultrafast X-ray Science facility at the ALS [15].

Acknowledgement

This work was supported by the Director, Office of Science, Office of Basic Energy Sciences, of the U.S. Department of Energy under Contract No. DE-AC03-76SF00098.

References

1. J. A. V. Vechten, R. Tsu, and F. W. Saris, "Nonthermal pulsed laser annealing of Si; Plasma annealing," *Physics Letters*, **74A**, 422-426, 1979.
2. P. Stampfli and K. H. Bennemann, "Time dependence of the laser-induced femtosecond lattice instability of Si and GaAs - role of longitudinal optical phonons," *Phys. Rev. B*, **49**, 7299-7305, 1994.
3. P. L. Silvestrelli, A. Alavi, M. Parrinello, and D. Frenkel, "Structural, dynamical, electronic, and bonding properties of laser-heated silicon: An ab initio molecular-dynamics study," *Phys. Rev. B*, **56**, 3806-3812, 1997.
4. C. V. Shank, R. Yen, and C. Hirlimann, "Time-resolved reflectivity measurement on femtosecond-optical-pulse-induced phase transitions on silicon," *Phys. Rev. Lett.*, **50**, 454-457, 1983.
5. H. W. K. Tom, G. D. Aumiller, and C. H. Brito-Cruz, "Time-resolved study of laser-induced disorder of Si surfaces," *Phys. Rev. Lett.*, **60**, 1438-1441, 1988.
6. K. Sokolowski-Tinten, H. Schulz, J. Bialkowski, and D. v. d. Linde, "Two distinct transitions in ultrafast solid-liquid phase transformations of GaAs," *Appl. Phys. A*, **53**, 227-234, 1991.
7. C. Rischel, A. Rousse, I. Uschmann, P.-A. Albouy, J.-P. Geindre, P. Audebert, J.-C. Gauthier, E. F:orster, J.-L. Martin, and A. Antonetti, "Femtosecond time-resolved X-ray diffraction from laser-heated organic films," *Nature*, **390**, 490-492, 1997.
8. C. W. Siders, A. Cavalleri, K. Sokolowski-Tinten, C. Toth, T. Guo, M. Kammler, M. Horn von Hoegen, K. R. Wilson, D. von der Linde, and C. P. J. Barty, "Detection of nonthermal melting by ultrafast X-ray diffraction," *Science*, **286**, 1340-1342., 1999.
9. R. W. Schoenlein, W. P. Leemans, A. H. Chin, P. Volfbeyn, T. E. Glover, P. Balling, M. Zolotorev, K.-J. Kim, S. Chattopadhyay, and C. V. Shank, "Femtosecond x-ray pulses at 0.4 angstroms generated by 90^{o} Thomson scattering: A tool for probing the structural dynamics of materials," *Science*, **274**, 236-238, 1996.

10. A. H. Chin, R. W. Schoenlein, T. E. Glover, P. Balling, W. P. Leemans, and C. V. Shank, "Ultrafast structural dynamics in InSb probed by time-resolved x-ray diffraction," *Phys. Rev. Lett.*, **83**, 336-339, 1999.
11. J. Larsson, Z. Chang, E. Judd, P. J. Schuck, R. W. Falcone, P. A. Heimann, H. A. Padmore, H. C. Kapteyn, P. H. Bucksbaum, M. M. Murnane, R. W. Lee, A. Machacek, J. S. Wark, X. Liu, and B. Shan, "Ultrafast X-ray diffraction using a streak-camera detector in averaging mode," *Opt. Lett.*, **22**, 1012, 1997.
12. A. M. Lindenberg, I. Kang, S. L. Johnson, T. Missalla, P. A. Heimann, Z. Chang, J. Larsson, P. H. Bucksbaum, H. C. Kapteyn, H. A. Padmore, R. W. Lee, J. S. Wark, and R. W. Falcone, "Time-resolved x-ray diffraction from coherent phonons during laser-induced phase transition," *Phys. Rev. Lett.*, **84**, 111-114, 2000.
13. A. A. Zholents and M. S. Zolotorev, "Femtosecond x-ray pulses of synchrotron radiation," *Phys. Rev. Lett.*, **76**, 912-915, 1996.
14. R. W. Schoenlein, S. Chattopadhyay, H. H. W. Chong, T. E. Glover, P. A. Heimann, C. V. Shank, A. Zholents, and M. Zolotorev, "Generation of femtosecond pulses of synchrotron radiation," *Science*, **287**, 2237-2240, 2000.
15. R. W. Schoenlein, S. Chattopadhyay, H. H. W. Chong, T. E. Glover, P. A. Heimann, C. V. Shank, A. Zholents, and M. Zolotorev, "Generation of x-ray pulses via laser-electron beam interaction," *Appl. Phys. B*, **71**, 1-10, 2000.

Figures

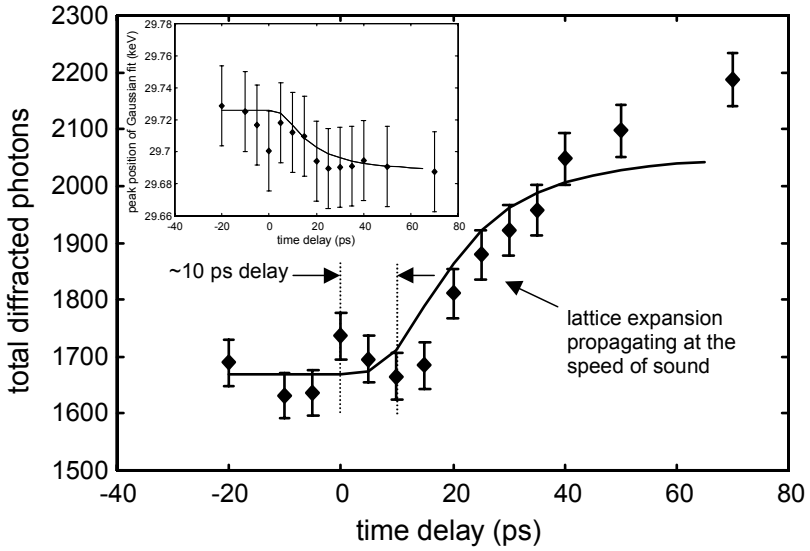

Figure 1. Diffracted x-ray photons (30 keV), integrated over the InSb Bragg peak, as a function of time delay following laser pulse excitation. Inset: time-dependent shift in spectral position of Bragg peak. Solid lines are from a model calculation accounting for energy transfer from an electron-hole plasma to LO phonons to acoustic phonon population and subsequent propagation of strain into the crystal [10].

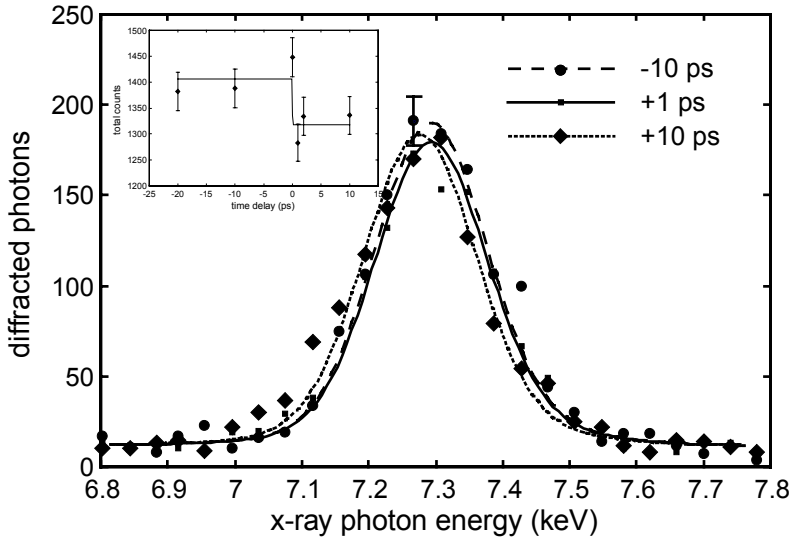

Figure 2. Representative x-ray diffraction spectra (with simulated profiles) for different time delays, taken with 7.3-keV x-rays. Inset: Normalized integrated x-ray diffracted photons as a function of time delay [10].

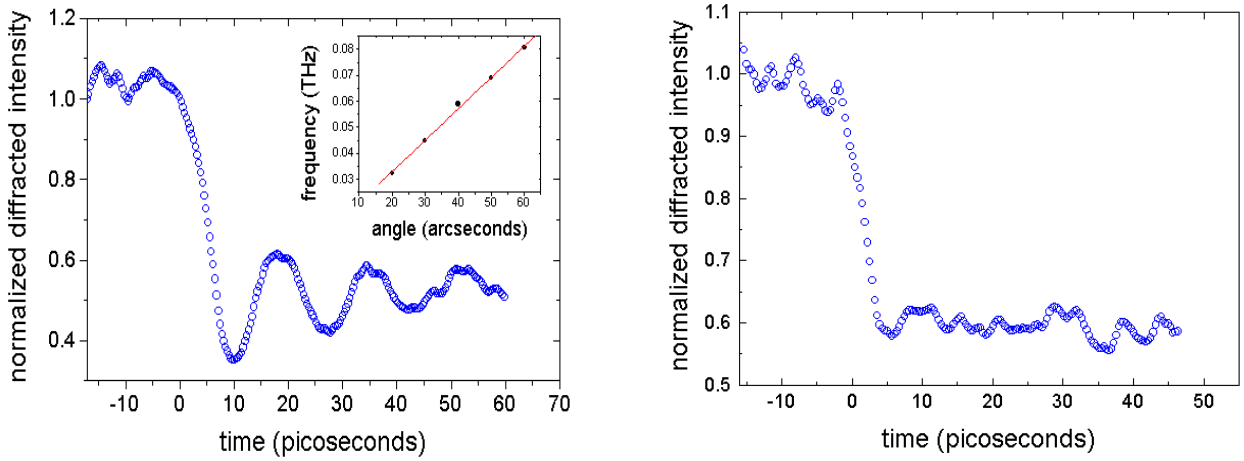

Figure 3. (left) Sinusoidal modulation of x-ray diffraction by coherent acoustic phonons measured at 40 arcsec away from the (111) Bragg peak of InSb. The inset shows the phonon frequencies measured at different angular deviations from the Bragg peak. (right) At higher fluence, rapid disordering is indicated by the prompt drop in the diffraction efficiency and absence of vibrational coherence [12].

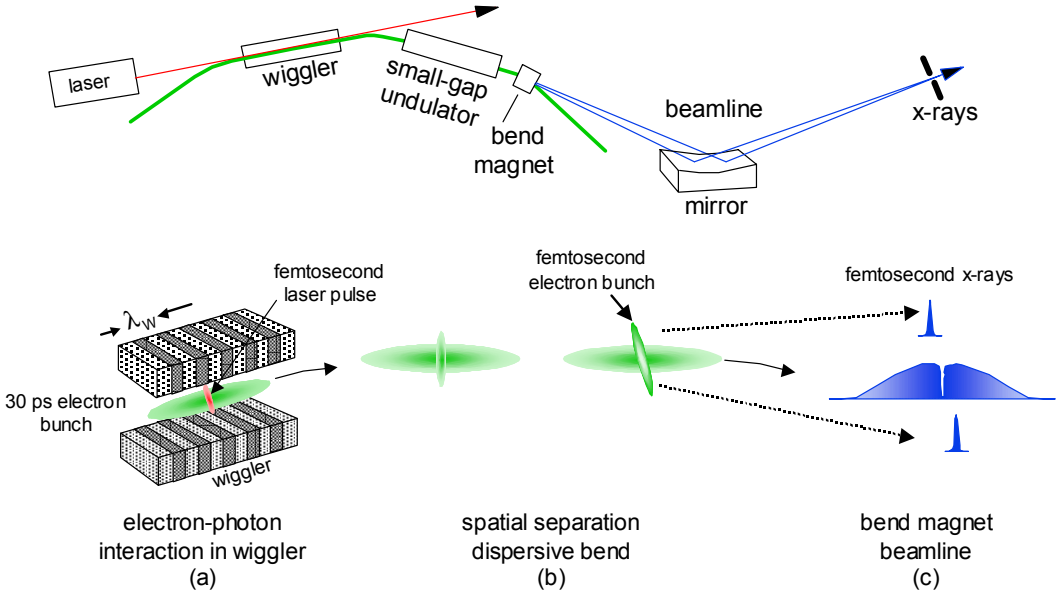

Figure 4. Schematic of method for generating femtosecond synchrotron pulses. (A) Femtosecond laser pulse interaction with the electron bunch in a resonantly-tuned wiggler. (B) Transverse separation of modulated electrons in a dispersive bend of the storage ring. (C) Generation of synchrotron radiation from a bend-magnet (or undulator) and separation of the femtosecond synchrotron radiation at the beamline image plane.

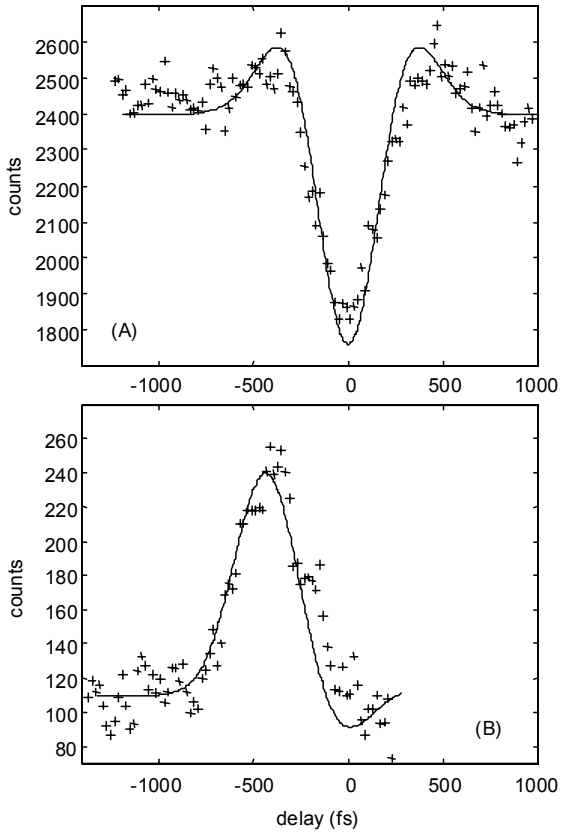

Figure 5. Cross-correlation measurements between a delayed laser pulse and synchrotron radiation originating from an energy-modulated electron bunch. In (A), synchrotron radiation from the central core ($\pm 3\sigma_x$) of the electron bunch is selected. In (B), synchrotron radiation from the horizontal wings ($+3\sigma_x$ to $+8\sigma_x$) of the electron bunch is selected. Solid lines are from a model calculation of the spatial and temporal distribution of the energy-modulated electron bunch following propagation through 1.5 arc-sectors at the ALS [15].

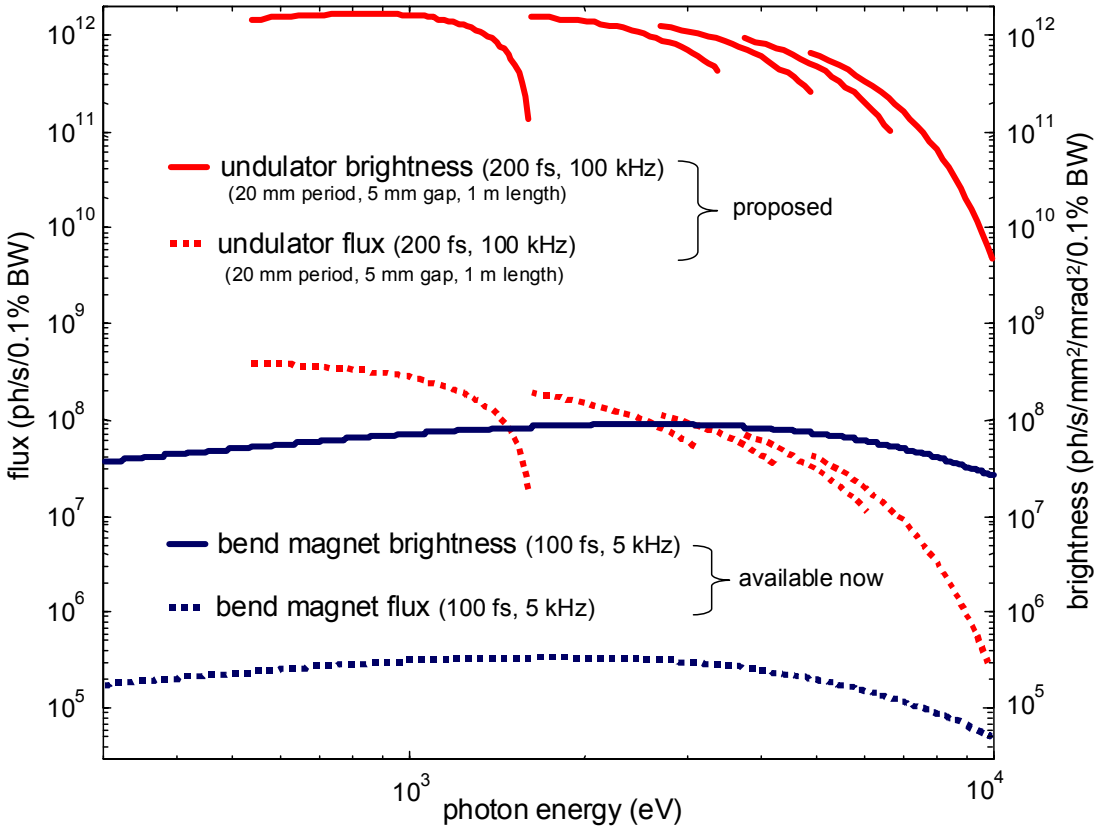

Figure 6. Flux and brightness for two femtosecond x-ray beamlines based on a bend-magnet and on an undulator. The undulator spectra is the locus of narrow spectral peaks (tuned by adjusting the undulator gap) and represents the envelope of harmonics 1, 3, 5, 7, and 9 [15].